Int. J. Solids Structures Vol. 23, No. 7, pp. 1003–1025, 1987
Printed in Great Britain.

0020-7683/87 $3.00+ .00

COUPLED DAMAGE AND MOISTURE-TRANSPORT IN FIBER-REINFORCED, POLYMERIC COMPOSITES

Y. WEITSMAN
Mechanics and Materials Center, Texas A&M University, College Station, TX 77843, U.S.A.

(*Received* 23 *April* 1986; *in revised form* 9 *October* 1986)

Abstract—This paper presents a mathematical model for the coupling between moisture diffusion and damage in fiber-reinforced, polymeric composites. In these materials, moisture was observed to cause damage by a multitude of minute debondings at the fiber–matrix interfaces. The model employs concepts of continuum damage theory to describe those debondings. Formal evolutionary expressions are derived and related to the extent of damage, the stress field, moisture content and moisture gradient. The effects of damage on moisture diffusion and on reductions in moduli are also formulated. Qualitative comparisons with experimental results are provided.

NOTATION

A	reference surface
A_{ij}	a generic symmetric second rank tensor
B_1–B_4	damage and moisture dependent coefficients
c_{po}, c_{pq}	damage and moisture dependent moduli
D	damage quantity, $d^2_{[31]} - d^2_{[32]}$
$D_{[PQ]}$	components of skew-symmetric damage tensor in reference configuration
$d_{[ij]}$	components of skew-symmetric damage tensor in deformed configuration
E_{KL}	Lagrangian strains
e_{ijk}, e_{IJK}	alternator tensor
F_A	flux of vapor mass in reference configuration
f_i	flux of vapor mass in deformed configuration
G_c	temperature gradients in reference configuration
g_i	temperature gradients in deformed configuration
H_1–H_9	coefficients in transversely isotropic vector valued functions
$\tilde{h}$	vapor's enthalpy in equilibrium reservoir
h_1–h_4	coefficients in skew-symmetric tensor valued functions
I_1–I_{23}	transversely isotropic invariants
m	vapor mass content
P_1–P_{23}	coefficients in transversely isotropic vector valued functions
$\tilde{p}$	vapor pressure in equilibrium reservoir
Q_A	heat flux vector in reference configuration
q_i	heat flux in deformed configuration
r_1–r_{14}	coefficients in skew-symmetric tensor valued functions
$r_{[ij]}$	affinities to rate of damage growth
S_{KL}	components of symmetric Kirchhoff stress
s	entropy density of solid–vapor mixture per unit solid mass
$\tilde{s}$	entropy density of vapor in equilibrium reservoir
T	temperature
u	energy density of solid–vapor mixture per unit solid mass
$\tilde{u}$	internal energy density of vapor in equilibrium reservoir
u_1–u_3	components of transversely isotropic vector valued functions
V	reference volume
V_i	a generic vector
v_i	velocity of solid particles
$W_{[ij]}$	a generic skew-symmetric tensor
X_i	position vector in reference configuration
x_i	position vector in deformed configuration
Z_B	moisture gradient in reference configuration
z_i	moisture gradient in deformed configuration.

Greek symbols

β_1–β_4	damage and moisture-dependent coefficients
γ_1–γ_{13}	
ε_{ij}	infinitesimal strains
$\chi_{[ij]}$	components of a transversely isotropic, skew-symmetric tensor valued function
$\tilde{\mu}$	chemical potential of vapor in equilibrium reservoir

μ_A	chemical potential of ambient vapor
$\tilde{\rho}$	vapor density in equilibrium reservoir
ρ_s	density of solid mass in deformed configuration
σ_{ij}	Cauchy stress
ϕ	Gibbs free energy
$\phi_{[ij]}, \Phi_{[ij]}$	components of rate of damage growth in deformed and reference configuration
ψ	Helmholz free energy

1. INTRODUCTION

It is well known that in many materials deformation under loads is associated with the formation of a multitude of internal flaws. These flaws, which may be microvoids, microcracks or microcrazes, precede the development of macrocracks which cause final failure. The above-mentioned flaws can be caused by environmental agents such as moisture and temperature, in addition to mechanical loads.

In the many circumstances where microflaws are distributed in a statistically homogeneous manner it is advantageous to represent them as internal state variables and employ thermodynamic considerations to establish constitutive relations and evolutionary expressions for flaw growth[1, 2]. This approach is employed by several "continuum damage" models which were reviewed recently by Krajcinovic[3]. Guided by various physical and mathematical considerations, the internal state variables were chosen as scalars, vectors, and tensors of various ranks. The case of a vector valued internal state variable was employed by Talreja[4, 5] to model damage in fiber-reinforced, composite laminates and relate stiffness reductions to external loads. More recently, a revision in the interpretation of "damage" as microcrack areas led to the selection of internal state variables as axial vectors (or, equivalently, as skew-symmetric tensors)[6]. This choice will also be employed in the present work.

Since the present investigation aims specifically at fibrous composites, where damage forms in characteristic patterns, the existence of a "representative damaged cell" is assumed. The components of the axial vector which represents "damage" are then defined as the projections of the total area of microcracks contained within the cell on its "walls". When those projections are divided by the respective areas of the cell's walls the measure of damage is nondimensional. The representation of all the microcracks within a cell by a single axial vector certainly obscures the distinction between a few "large" microcracks and many smaller microcracks. However, in circumstances when damage forms in consistent patterns such a distinction may not be important because the variability in microcrack sizes is likely to be limited. The interactions between microcracks within the cell will certainly depend on the external loads. It will be shown that the present model accounts for this dependence through stress-related damage evolution relations.

With few exceptions[7], most existing continuum damage formulations employ linearization in the damage parameters. By contrast, the present formulation does not involve series expansions in the damage parameter and is not limited to "small" damage.

In the presence of sharp gradients of temperature or moisture content, the expansional strains may be highly nonuniform within the characteristic damaged cell. In this case the stresses are likely to vary even along each of the individual microcracks, resulting in elevated stress-intensity factors at the microcrack tips. Within the context of a continuum damage theory these increases in stress intensity are reflected in gradient-dependent damage evolution relations. Such relations are also considered in this paper.

The effects of moisture in polymeric composites were investigated over more than a decade. A comprehensive review which appeared recently[8] listed more than 300 references on the subject. Damage due to moisture, which developed as debondings at the fiber–matrix interfaces, was observed by several investigators[9–17]. This typical form of moisture-induced damage was attributed to the presence of hygrophilic chemical agents at the fibers' surfaces[9]. Since the epoxy may act as a semi-permeable membrane, the high concentrations of moisture result in excessive osmotic pressures at the interfaces, leading to fiber–matrix debondings.

In another study[18] it was shown that epoxy resins absorbed excessive contents of moisture when the amount of curing agent in the mixture was below stoichiometry. Since it is plausible to assume that the stoichiometry of the resin would change in the vicinity of the fiber interfaces it is conceivable that the interphase regions contain excessive levels of moisture, which cause interfacial cracking.

The process of moisture sorption is associated with a thermodynamically "open" system, since vapor mass is being added to the material volume of the composite. This process will be accommodated in this paper by considering a hypothetical vapor reservoir which is in thermodynamic equilibrium with the actual vapor contained in a material volume-element of the composite.

This approach follows the ideas employed by Biot[19–21] in connection with flow through porous media. It should be pointed out that in spite of the similarity between Biot's approach and the present formulation the two are not identical. The natural internal variable in Biot's scheme is the pore pressure, while in the present work it is more suitable to employ moisture content, or alternately the chemical potential. The subtle differences between the two formulations were pointed out by Gurtin[22].

2. BASIC EQUATIONS

Consider a solid body B occupying a material volume V bounded by a surface A. Let the solid, of mass density ρ_s, absorb vapor through its boundary and let m denote the vapor mass per unit volume of the solid. Also, let $\mathbf{x}$ be the position of a solid mass particle in the deformed configuration that corresponds to the place $\mathbf{X}$ in the undeformed state, and let $\mathbf{f}$, $\mathbf{q}$ and $\mathbf{v}$ denote fluxes of vapor mass and of heat, and the velocity of the solid particles, respectively.

In addition, let u and s be the internal energy and entropy densities of the solid–vapor mixture per unit solid mass, and let σ_{ij} and T denote the components of the Cauchy stress and temperature, respectively.

A proper accounting of the state of the solid/vapor mixture, which is a thermodynamically open system, is obtained by considering each element in thermodynamic equilibrium with a reservoir containing vapor at pressure $\tilde{p}$, density $\tilde{\rho}$, and internal energy and entropy densities $\tilde{u}$ and $\tilde{s}$, respectively[20, 23, 24].

Conservation of the solid and vapor masses gives

$$\dot{\rho}_s + \rho_s \nabla \cdot \mathbf{v} = 0 \tag{1}$$

$$\dot{m} = -\nabla \cdot \mathbf{f}. \tag{2}$$

Conservation of energy over B reads

$$\frac{\mathrm{d}}{\mathrm{d}t}\int_V \rho_s u \, \mathrm{d}V = \int_A \sigma_{ij} n_j v_i \, \mathrm{d}A - \int_A q_i n_i \, \mathrm{d}A - \int_A \tilde{p}\frac{f_i}{\tilde{\rho}} n_i \, \mathrm{d}A - \int_A \tilde{u} f_i n_i \, \mathrm{d}A. \tag{3}$$

The third integral on the right-hand side of eqn (3) expresses the mechanical power due to vapor flux, observing that $f_i/\tilde{\rho}$ corresponds to vapor velocity. The last integral in eqn (3) expresses the rate of vapor-borne energy.

The entropy inequality reads

$$\frac{\mathrm{d}}{\mathrm{d}t}\int_V \rho_s s \, \mathrm{d}V \geqslant \int_A -(q_i/T) n_i \, \mathrm{d}A - \int_A \tilde{s} f_i n_i \, \mathrm{d}A \tag{4}$$

where the last integral in eqn (4) expresses the rate of vapor-borne entropy.

Application of Green's theorem to eqns (3) and (4), and using eqn (2), yields

$$\rho_s \dot{u} = \sigma_{ij} v_{i,j} - q_{i,i} - \tilde{h}_{,i} f_i + \tilde{h}\dot{m} \tag{5}$$

and

$$\rho_s T\dot{s} \geqslant -q_{i,i} + (q_i/T) g_i - T\tilde{s}_{,i} f_i + T\tilde{s}\dot{m} \tag{6}$$

where $\tilde{h} = (\tilde{p}/\tilde{\rho}) + \tilde{u}$ is the enthalpy of the vapor in the hypothetical reservoir and $g_i = T_{,i}$.

Elimination of $q_{i,i}$ between eqns (5) and (6) yields the following expression for the "reduced entropy inequality"

$$-\rho_s \dot{\psi} - \rho_s s\dot{T} + \sigma_{ij} v_{i,j} - (q_i/T) g_i + \tilde{\mu}\dot{m} - f_i \tilde{\mu}_{,i} - \tilde{s} g_i f_i \geqslant 0. \tag{7}$$

In inequality (7) $\psi = u - Ts$ is the Helmholz free energy and $\tilde{\mu} = \tilde{h} - T\tilde{s}$ is the chemical potential of the vapor in the hypothetical reservoir.

3. DISTRIBUTED DAMAGE

When materials possess a statistically homogeneous microstructure, their mechanical response is associated with the creation and growth of a multitude of internal flaws. For several types of material microstructure these microflaws develop in characteristic patterns, until they finally coalesce to form a localized, dominant crack whose growth leads to ultimate failure. Some characteristic damage patterns are shown in Figs 1 and 2 for fibrous composite laminates of different lay-ups[25, 26]. Patterned damage was also observed in concrete and in ceramic materials.

In the above-mentioned circumstances it is possible to relate the distributed flaws to a characteristic material "cell" and express the damage by means of a continuous, internal state variable[27]. Such cells are overlaid on the damage patterns in Figs 1 and 2.

For damage due to microcracking, the internal state variable can be selected to represent the projections of all microcrack surfaces on the "walls" of the characteristic cell. Since areas are expressed as vector products of directed line-segments, the present choice leads to a mathematical representation of "damage" as a skew-symmetric, second rank tensor $d_{[ij]}$. The quantity $d_{[ij]}$ may be viewed as nondimensional, since it can be formed by dividing all projected microcrack areas through the respective areas of the cell walls.

In the presence of hygrothermal effects, diffusion and damage phenomena are likely to depend on gradients of moisture content $\partial m/\partial x_i$ and of the temperature $\partial T/\partial x_i$. Upon consideration of the above-mentioned characteristic cell it is possible to relate the latter dependencies to non-dimensional gradients $\partial m/\partial \xi_i$ and $\partial T/\partial \xi_i$, where $\xi_i = x_i/L_i$ (no sum on i), with L_i being the lengths of the cell sides[27].

Finally, it should be noted that each microcrack is contained within two equal and opposite surfaces. Consequently, the constitutive formulation which employs $d_{[ij]}$ as an internal state variable should remain insensitive to the sign of $d_{[ij]}$.

4. ELASTIC RESPONSE WITH DISTRIBUTED DAMAGE

Consider the response of elastic materials with distributed internal damage. In addition, let the material be exposed to thermal effects and absorb moisture from the ambient environment.

In these circumstances the list of internal state variables contains the deformation gradients $F_{iJ} = \partial x_i/\partial X_J$, "damage" $d_{[ij]}$, moisture m, temperature T and the gradients $z_i = \partial\tilde{\mu}/\partial x_i$ and $g_i = \partial T/\partial x_i$ of the chemical potential $\tilde{\mu}$ and of T. As noted earlier, both gradients and $d_{[ij]}$ may be viewed as nondimensional, while F_{iJ} is obviously dimensionless. In addition, T and $\tilde{\mu}$ can be nondimensionalized as well by dividing their actual values through some reference levels.

Considerations of frame indifference and employment of the reduced entropy inequality[28] give

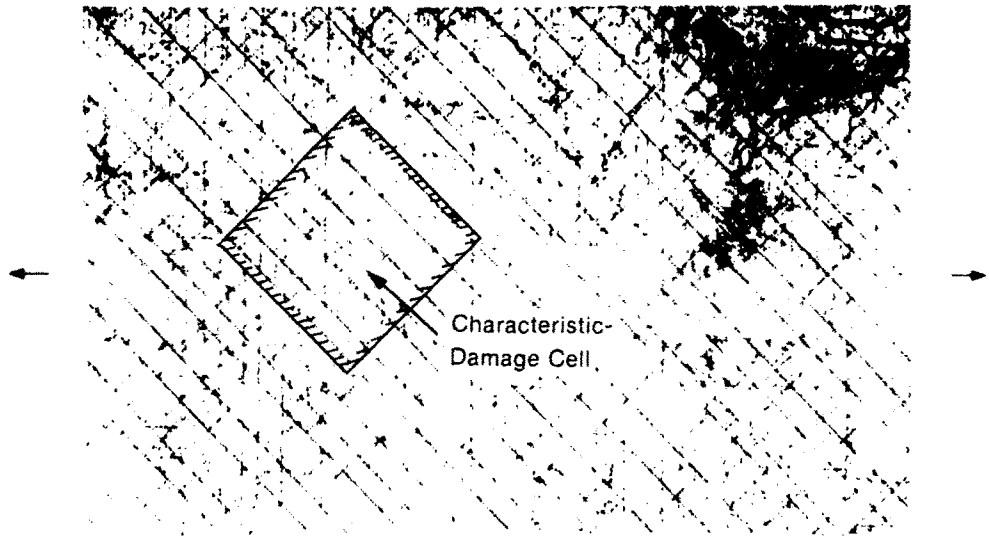

Fig. 1. A radiograph showing the pattern of matrix cracks in a $[0, 90, \pm 45]_S$ graphite/epoxy laminate[26]. The "characteristic-damage cell" is superimposed.

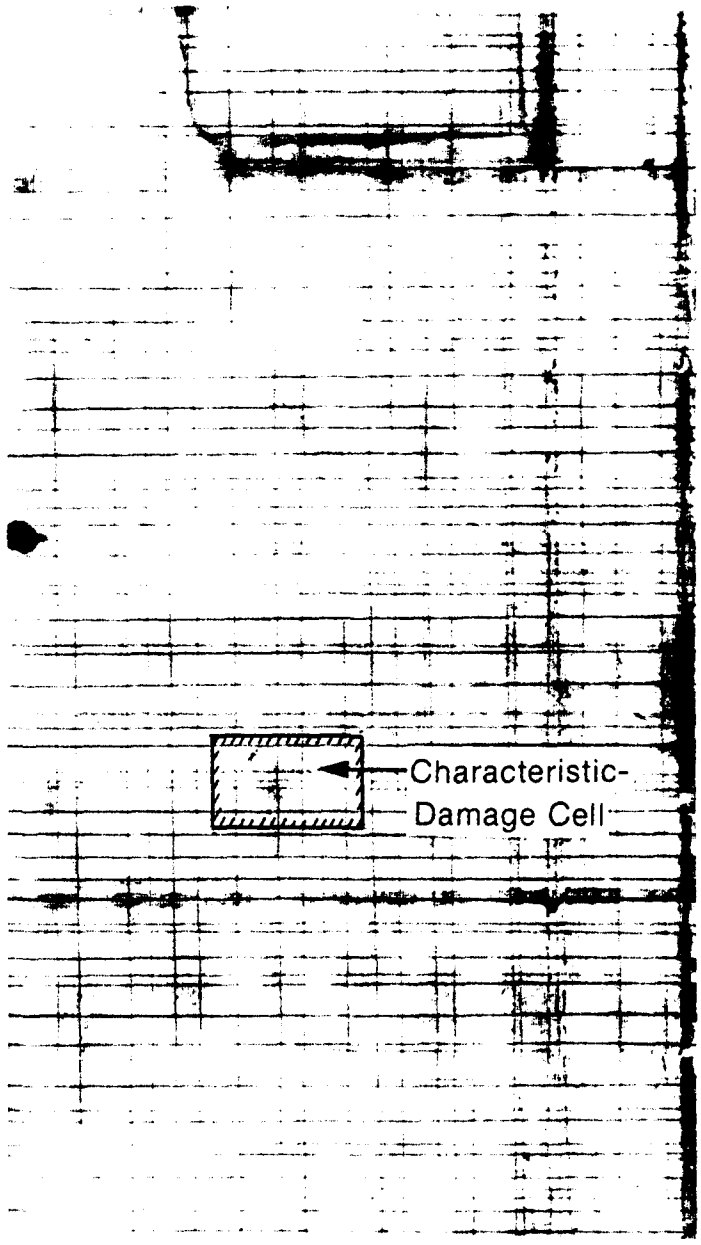

Fig. 2. A radiograph showing the pattern of matrix cracking in a $[0, 90_2]_S$ graphite/epoxy laminate[25]. The "characteristic-damage cell" is superimposed.

$$\psi = \psi^*(E_{KL}, D_{[PQ]}, m, T) \tag{8}$$

$$s = -\frac{\partial \psi^*}{\partial T} \tag{9a}$$

$$\tilde{\mu} = \rho_s \frac{\partial \psi^*}{\partial m} \tag{9b}$$

$$S_{KL} = \frac{\partial(\rho_s \psi^*)}{\partial E_{KL}} \tag{9c}$$

and

$$\tilde{\mu}_{,i} f_i + g_i(q_i/T + \tilde{s} f_i) + r_{[ij]}\phi_{[ij]} \leqslant 0 \tag{10}$$

where $\psi = u - Ts$ is the Helmholz free energy, $E_{KL} = \frac{1}{2}(F_{iK}F_{iL} - \delta_{KL})$ are the Lagrangian strain components, S_{KL} are the components of the symmetric Kirchhoff stress[29], $D_{[PQ]}$ are the components of the damage variable $d_{[ij]}$ referred to the undeformed configuration. Since both $d_{[ij]}$ and $D_{[PQ]}$ are areas they are related by

$$d_{[ij]} = JX_{L,k}e_{kji}e_{LPQ}D_{[PQ]} \tag{11}$$

with $J = \det \partial x_i/\partial X_K$.

In addition, in eqn (10), $r_{[ij]}$ is the "affinity" to the rate of damage growth $\phi_{[ij]} = \dot{d}_{[ij]}$, namely

$$r_{[ij]} = \rho_s \frac{\partial \psi^*}{\partial d_{[ij]}}. \tag{12}$$

Furthermore, we obtain the following forms for the fluxes

$$Q_A = Q_A^*(E_{KL}, D_{[PQ]}, G_c, Z_B, T, m) \tag{13a}$$

$$F_A = F_A^*(E_{KL}, D_{[PQ]}, G_c, Z_B, T, m) \tag{13b}$$

$$\Phi_{[IJ]} = \Phi_{[IJ]}^*(E_{KL}, D_{[PQ]}, G_c, Z_B, T, m). \tag{13c}$$

In eqns (13) Q_A, F_A, and $\Phi_{[IJ]}$ are components of heat and moisture flux and of rate of damage growth in the reference coordinates X_A. They are related to q_i and f_i through $Q_A = X_{A,i}q_i$, $F_A = X_{A,i}f_i$ and $\Phi_{[IJ]}$ is expressible in terms of $\phi_{[ij]}$ in the same manner as given in eqn (11) for $D_{[IJ]}$ and $d_{[ij]}$. In addition G_c and Z_B are gradients referred to the undeformed configuration, namely $G_C = x_{i,C}g_i$ and $Z_B = x_{i,B}z_i$[7].

To simplify the subsequent formulation we shall restrict ourselves to isothermal conditions. In this case $g_i = 0$, whereby

$$F_A = \hat{F}_A(E_{KL}, D_{[PQ]}, Z_B, m; T_0) \tag{14a}$$

and

$$\Phi_{[IJ]} = \hat{\Phi}_{[IJ]}(E_{KL}, D_{[PQ]}, Z_B, m; T_0). \tag{14b}$$

In addition, inequality (10) reduces to

$$\tilde{\mu}_{,i} f_i + r_{[ij]}\phi_{[ij]} \leqslant 0. \tag{15}$$

5. FIBER-REINFORCED MATERIALS. TRANSVERSE ISOTROPY

Consider unidirectionally reinforced fibrous materials. Such substances are transversely isotropic about, say, the x_3-axis and, in the absence of any right-handed or left-handed internal structure, possess also reflective symmetries in the x_1- and x_3-axes.†

To derive the detailed dependencies of ψ, F_A and $\Phi_{[IJ]}$ on E_{KL}, $D_{[PQ]}$ and Z_B it is necessary to form all the transversely isotropic invariants among these variables[30].

The complete list is given in the Appendix, where A_{ij}, W_{ij} and V_i denote a symmetric second rank tensor, a skew-symmetric second rank tensor, and a vector, respectively.

Note that the Appendix lists 33 invariants. However, the 13 invariants I_6, I_{11}, I_{15}, I_{18}, I_{20}, I_{21}, I_{23}, I_{24}, I_{25}, I_{27}, I_{29}, I_{30}, I_{32} are *odd* in W_{ij} and therefore inadmissible to represent damage that must remain insensitive to the sign of $d_{[ij]}$. This leaves 20 invariants for expressing F_A and $\Phi_{[IJ]}$, as explained in the sequel.‡

In view of eqn (8), the free energy ψ depends only on E_{KL} and $D_{[PQ]}$. Consequently, the scalar ψ depends only on the ten invariants I_1–I_5, I_9, I_{10}, I_{12}, I_{19} and I_{22}.‡

Expressions for F_A are obtained by considering the integrity basis for one symmetric and one skew-symmetric second rank tensor and *two* vectors under T-4 symmetry, subsequently retaining only those terms which are linear in the second vector[31, 32]. The results of this procedure are listed in the Appendix, where the components of the vector valued function $\mathbf{U}$: u_1, u_2, u_3 are related to those of A_{ij}, W_{ij} and V_i. The 32 terms P_1–P_{23}, H_1–H_9 in the expressions for (u_1, u_2) and u_3 are functions of the 20 invariants I_1–I_5, I_7–I_{10}, I_{12}–I_{14}, I_{16}, I_{17}, I_{19}, I_{22}, I_{26}, I_{28}, I_{31} and I_{33} formed among A_{ij}, W_{ij} and V_i.

In view of the fact that the flux components F_A must remain insensitive to the sign of the damage variable $d_{[ij]}$ it is necessary to discard all terms odd in W_{ij}, hence $P_3 = P_5 = P_8 = P_9 = P_{11} = P_{13} = P_{14} = P_{15} = P_{17} = P_{19} = P_{20} = P_{22} = H_3 = H_5 = H_6 = H_8 = 0$. This leaves only 16 terms out of the original list of 32 terms P_1–P_{23}, H_1–H_9.

Expressions for $\Phi_{[IJ]}$ are obtained by considering the integrity basis for one symmetric second rank tensor, one vector and *two* skew-symmetric second rank tensors under T-4 symmetry, then retaining only those terms which are linear in the second skew-symmetric tensor. In this manner a list of terms is generated, which contains products of components of A_{ij}, W_{ij} and V_i with one component of the second skew-symmetric tensor, say $Y_{[mn]}$. At this stage generate a second list of terms by transposing the indices m and n, namely by forming scalar components of transposed terms among A_{ij}, W_{ij} and V_i that correspond to $Y_{[nm]}$.

The desired skew-symmetric tensor valued functions are then obtained by subtracting the factors that multiply $Y_{[mn]}$ from those which multiply $Y_{[nm]}$.

The results of this procedure are given in the Appendix, where $\chi_{[31]}$, $\chi_{[32]}$ and $\chi_{[12]}$ are related to components of A_{ij}, W_{ij} and V_i. The 18 terms r_1–r_{14}, h_1–h_4 in the Appendix are functions of the same 20 invariants I_1–I_5, I_7–I_{10}, I_{12}–I_{14}, I_{16}, I_{17}, I_{19}, I_{22}, I_{26}, I_{28}, I_{31} and I_{33} that enter P_1, P_2, etc. Note that the process of transposition from $Y_{[mn]}$ to $Y_{[nm]}$ and subsequent subtraction automatically eliminates all terms odd in W_{ij} from the list for $\chi_{[IJ]}$, hence no further reduction is necessary to account for sign insensitivity to the damage parameter $d_{[ij]}$.

6. INFINITESIMAL DEFORMATIONS. STRAIN FORMULATION

Consider infinitesimal deformations. In this case $E_{IJ} \to \varepsilon_{ij}$, $S_{KL} \to \sigma_{kl}$, $F_I \to f_i$, $D_{[MN]} \to d_{[mn]}$ and $\rho_s \simeq \rho_{s0}$ (constant).

Expanding the free energy in powers of ε_{ij}, truncating after the second power, we get

$$\begin{aligned}\rho_{s0}\psi = {} & \psi_0 + \beta_1\varepsilon_{33} + \beta_2(\varepsilon_{11}+\varepsilon_{22}) + \beta_3[D(\varepsilon_{11}-\varepsilon_{22}) + 4d_{[31]}d_{[32]}\varepsilon_{12}] \\ & + \beta_4 d_{[12]}(\varepsilon_{31}d_{[32]} - \varepsilon_{32}d_{[31]}) + \gamma_1\varepsilon_{33}^2 + \gamma_2(\varepsilon_{11}+\varepsilon_{22})^2 \\ & + \gamma_3[D(\varepsilon_{11}-\varepsilon_{22}) + 4d_{[31]}d_{[32]}\varepsilon_{12}]^2\end{aligned}$$

† These combined symmetries are denoted by the class T-4 in Ref. [30].
‡ See, however, Addendum.

$$
\begin{aligned}
&+\gamma_4 d_{[12]}^2(\varepsilon_{31}d_{[32]}-\varepsilon_{32}d_{[31]})^2+\gamma_5\varepsilon_{33}(\varepsilon_{11}+\varepsilon_{22})\\
&+\gamma_6\varepsilon_{33}[D(\varepsilon_{11}-\varepsilon_{22})+4d_{[31]}d_{[32]}\varepsilon_{12}]\\
&+\gamma_7\varepsilon_{33}d_{[12]}(\varepsilon_{31}d_{[32]}-\varepsilon_{32}d_{[31]})\\
&+\gamma_8(\varepsilon_{11}+\varepsilon_{22})[D(\varepsilon_{11}-\varepsilon_{22})+4d_{[31]}d_{[32]}\varepsilon_{12}]\\
&+\gamma_9(\varepsilon_{11}+\varepsilon_{22})d_{[12]}(\varepsilon_{31}d_{[32]}-\varepsilon_{32}d_{[31]})\\
&+\gamma_{10}[D(\varepsilon_{11}-\varepsilon_{22})+4d_{[31]}d_{[32]}\varepsilon_{12}]d_{[12]}(\varepsilon_{31}d_{[32]}-\varepsilon_{32}d_{[31]})\\
&+\gamma_{11}[(\varepsilon_{11}-\varepsilon_{22})^2+4\varepsilon_{12}^2]+\gamma_{12}(\varepsilon_{31}^2+\varepsilon_{32}^2)\\
&+\gamma_{13}d_{[12]}[(\varepsilon_{11}-\varepsilon_{22})(\varepsilon_{31}d_{[32]}+\varepsilon_{32}d_{[31]})-2\varepsilon_{12}(\varepsilon_{31}d_{[31]}-\varepsilon_{32}d_{[32]})] \qquad (16)\dagger
\end{aligned}
$$

where ψ_0, β_i $(i=1,\ldots,4)$, γ_i $(i=1,\ldots,13)$ are functions of m, $d_{[31]}^2+d_{[32]}^2$, $d_{[12]}^2$, and T_0. Also $D=d_{[31]}^2-d_{[32]}^2$.

Stress–strain relations are obtainable from $\sigma_{ij}=\rho_{s0}(\partial\psi/\partial\varepsilon_{ij})$, where ε_{ij} is considered independent of ε_{ji}. Consequently, it is necessary to express all shear strains ε_{ij} $(i\neq j)$ in eqn (16) by $\frac{1}{2}(\varepsilon_{ij}+\varepsilon_{ji})$. Upon performing this modification, and then employing the "truncated" notation, with $\sigma_{11}\to\sigma_1$, $\sigma_{22}\to\sigma_2$, $\sigma_{33}\to\sigma_3$, $\sigma_{23}\to\sigma_4$, $\sigma_{31}\to\sigma_5$, $\sigma_{12}\to\sigma_6$ and $\varepsilon_{11}\to\varepsilon_1$, $\varepsilon_{22}\to\varepsilon_2$, $\varepsilon_{33}\to\varepsilon_3$, $2\varepsilon_{23}\to\varepsilon_4$, $2\varepsilon_{31}\to\varepsilon_5$, and $2\varepsilon_{12}\to\varepsilon_6$, we obtain

$$\sigma_p=C_{po}+C_{pq}\varepsilon_q\dagger \quad \text{where} \quad C_{pq}=C_{qp}. \qquad (17)$$

In eqn (17), we have

$$
\begin{aligned}
&C_{10}=\beta_2+\beta_3 D, \quad C_{20}=\beta_2-\beta_3 D, \quad C_{30}=\beta_1,\\
&C_{40}=-\tfrac{1}{2}\beta_4 d_{[12]}d_{[31]}, \quad C_{50}=\tfrac{1}{2}\beta_4 d_{[12]}d_{[32]},\\
&C_{60}=2\beta_3 d_{[31]}d_{[32]}
\end{aligned}
$$

and

$$
\begin{aligned}
&C_{11}=2(\gamma_2+\gamma_3 D^2+\gamma_8 D+\gamma_{11}), \qquad C_{12}=2(\gamma_2-\gamma_3 D^2-\gamma_{11}),\\
&C_{13}=\gamma_5+\gamma_6 D, \qquad C_{14}=\tfrac{1}{2}(-\gamma_9-\gamma_{10}D+\gamma_{13})d_{[12]}d_{[31]},\\
&C_{15}=\tfrac{1}{2}(\gamma_9+\gamma_{10}D+\gamma_{13})d_{[12]}d_{[32]}, \qquad C_{16}=2(2\gamma_3 D+\gamma_8)d_{[31]}d_{[32]},\\
&C_{22}=2(\gamma_2+\gamma_3 D^2-\gamma_8 D+\gamma_{11}), \qquad C_{23}=\gamma_5-\gamma_6 D,\\
&C_{24}=\tfrac{1}{2}(-\gamma_9+\gamma_{10}D-\gamma_{13})d_{[12]}d_{[31]}, \qquad C_{25}=\tfrac{1}{2}(\gamma_9-\gamma_{10}D-\gamma_{13})d_{[12]}d_{[32]},\\
&C_{26}=2(-2\gamma_3 D+\gamma_8)d_{[31]}d_{[32]}, \qquad C_{33}=2\gamma_1, \qquad C_{34}=\frac{-\gamma_7}{2}d_{[12]}d_{[31]},\\
&C_{35}=\frac{\gamma_7}{2}d_{[12]}d_{[32]}, \qquad C_{36}=2\gamma_6 d_{[31]}d_{[32]}, \qquad C_{44}=\gamma_4 d_{[12]}^2 d_{[31]}^2+\tfrac{1}{2}\gamma_{12},\\
&C_{45}=-\gamma_4 d_{[12]}^2 d_{[31]}d_{[32]}, \qquad C_{46}=-\gamma_{10}d_{[31]}^2 d_{[32]}d_{[12]}+\frac{\gamma_{13}}{2}d_{[12]}d_{[32]},\\
&C_{55}=\gamma_4 d_{[12]}^2 d_{[32]}^2+\frac{\gamma_{12}}{2}, \qquad C_{56}=\left(\gamma_{10}d_{[32]}^2-\frac{\gamma_{13}}{2}\right)d_{[12]}d_{[31]},\\
&C_{66}=2(4\gamma_3 d_{[31]}^2 d_{[32]}^2+\gamma_{11}).
\end{aligned}
$$

Note that when all $d_{[ij]}$ vanish the stress–strain relations reduce to the familiar

† See Addendum.

expressions for transverse isotropy about the x_3-axis. However, in the presence of damage the stiffness matrix C_{pq} contains all 21 components, all of which depend on $d_{[ij]}$. Obviously, all stiffness components may depend also on m and T_0.

For $\varepsilon_{ij} \ll 1$ we neglect all terms that involve the symmetric second rank tensor in the Appendix and obtain the following expressions for the vector that represents the moisture flux $\mathbf{f}$:

$$\begin{aligned} f_1 &= P_1 z_1 + P_6[(d_{[31]}^2 - d_{[32]}^2)z_1 + 2d_{[31]}d_{[32]}z_2] \\ f_2 &= P_1 z_2 + P_6[-(d_{[31]}^2 - d_{[32]}^2)z_2 + 2d_{[31]}d_{[32]}z_1] \\ f_3 &= H_1 z_3 + H_7 d_{[12]}(d_{[31]}z_2 - d_{[32]}z_1). \end{aligned} \tag{18}$$

In eqns (18) P_1, P_6, H_1 and H_7 are functions of the 20 invariants I_1–I_5, I_7–I_{10}, I_{12}–I_{14}, I_{16}, I_{17}, I_{19}, I_{22}, I_{26}, I_{28}, I_{31} and I_{33} formed from the components of the symmetric tensor ε_{ij}, the skew-symmetric tensor $d_{[ij]}$ and the vector z_i. Obviously P_1, P_6, H_1 and H_7 may depend also on m and on the (constant) temperature T_0.

Recall, however, that basic considerations of irreversible thermodynamics—as derived from the kinetic theory of gases—require that all coefficients in the flux–force relationships for transport terms should depend only on equilibrium state variables[33]. If this requirement were to be extended to solids as well then P_1, P_6, H_1 and H_7 in eqns (18) cannot depend on moisture gradients and hence can at most be functions of the ten invariants I_1–I_5, I_{10}, I_{12}, I_{14}, I_{19}, and I_{22}.

Note that the expansion of ψ in a power series of ε_{ij} does *NOT* imply that an analogous expansion must exist for P_1, P_6, H_1 and H_7. The present formulation therefore retains the option to consider non-linear coupling between mechanical fields and moisture flux[34].

Finally, employing similar arguments, we obtain the following expressions for the damage growth rates $\phi_{[ij]} = \dot{d}_{[ij]}$:

$$\begin{aligned} \phi_{[12]} &= h_1 d_{[12]} + h_4(d_{[31]}z_2 - d_{[32]}z_1)z_3 \\ \phi_{[31]} &= r_1 d_{[31]} + r_4[(z_1^2 - z_2^2)d_{[31]} + z_2(z_1 d_{[32]} - z_3 d_{[12]})] \\ &\quad + r_{11}d_{[12]}d_{[31]}z_1 z_2 + r_{13}(d_{[12]}z_3 - d_{[32]}z_1)z_2 \\ \phi_{[32]} &= r_1 d_{[32]} + r_4[-(z_1^2 - z_2^2)d_{[32]} + z_1(z_2 d_{[31]} - z_3 d_{[21]}) \\ &\quad - r_{11}d_{[12]}d_{[32]}z_1 z_2 - r_{13}(d_{[12]}z_3 - d_{[13]}z_2)z_1. \end{aligned} \tag{19}$$

In eqns (19), the terms h_1, h_4, r_1, r_4, r_{11} and r_{13} are functions of the same invariants as P_1, P_6, H_1, and H_7 above. Note that the terms h_1 and r_1 correspond to "self similar" damage growth, while the remaining functions h_4, r_4, r_{11} and r_{13} are associated with the "tilting" of microdamage due to gradients of the chemical potential.

7. INFINITESIMAL DEFORMATION. STRESS FORMULATION

Define the Gibbs free energy $\phi(\sigma_{ij}, d_{[ij]}, m; T_0)$ by

$$\rho_{s0}\phi = \rho_{s0}\psi - \sigma_{ij}\varepsilon_{ij}. \tag{20}$$

Then, in analogy with eqns (9) we have

$$\varepsilon_{ij} = -\rho_{s0}\frac{\partial \phi}{\partial \sigma_{ij}} \tag{21a}$$

$$s = -\frac{\partial \phi}{\partial T} \tag{21b}$$

$$\tilde{\mu} = \rho_{s0}\frac{\partial \phi}{\partial m}. \tag{22}$$

The "reduced entropy inequality", eqn (10), remains unchanged, except that now

$$r_{[ij]} = \rho_{s0}\frac{\partial \phi}{\partial d_{[ij]}}. \tag{23}$$

Consider a characteristic material stress, e.g. a failure stress σ_f, then for sufficiently small stresses (such that $\sigma_{ij}/\sigma_f \ll 1$) we can expand ϕ in powers of σ_{ij} and truncate after the second powers. This expansion has the same form as eqn (16), except that σ_{ij} replaces ε_{ij}, expansional coefficients $(-B_i)$ replace β_i, and compliances $(-\eta_i)$ replace the stiffness γ_i. An analogous procedure yields linear strain–stress relations similar to those given in eqn (17)

$$\varepsilon_p = S_{po} + S_{pq}\sigma_q \tag{24}$$

with S_{po} and S_{pq} the same as C_{po} and C_{pq} except that B_i and η_i appear in place of β_i and γ_i. In addition, expressions (18) and (19) also remain unchanged, except that P_1, P_6, H_1, H_7, h_1, h_4, r_1, r_4, r_{11} and r_{13} depend on 20 invariants that contain σ_{ij} in place of ε_{ij}.

In view of eqn (22), the chemical potential $\tilde{\mu}$ is given by

$$\begin{aligned}\tilde{\mu} = \rho_{s0}\frac{\partial \phi}{\partial m} = \frac{\partial \phi_0}{\partial m} &- \frac{\partial B_1}{\partial m}\left(\frac{\sigma_{33}}{\sigma_f}\right) - \frac{\partial B_2}{\partial m}\left(\frac{\sigma_{11}+\sigma_{22}}{\sigma_f}\right)\\ &- \frac{\partial B_3}{\partial m}\left[D\left(\frac{\sigma_{11}-\sigma_{22}}{\sigma_f}\right) + 4d_{[31]}d_{[32]}\left(\frac{\sigma_{12}}{\sigma_f}\right)\right]\\ &- \frac{\partial B_4}{\partial m}d_{[12]}\left[d_{[32]}\left(\frac{\sigma_{31}}{\sigma_f}\right) - d_{[31]}\left(\frac{\sigma_{32}}{\sigma_f}\right)\right]\\ &+ \text{higher-order terms in } (\sigma_{ij}/\sigma_f).\end{aligned} \tag{25}$$

For constant stresses the fluxes $z_i = \partial\tilde{\mu}/\partial x_i$ are given by

$$\begin{aligned}z_i = \rho_{s0}\Bigg[\frac{\partial^2 \phi}{\partial m^2}\frac{\partial m}{\partial x_i} &+ 2\frac{\partial^2 \phi}{\partial m\,\partial(d_{[31]}^2 + d_{[32]}^2)}\left(d_{[31]}\frac{\partial d_{[31]}}{\partial x_i} + d_{[32]}\frac{\partial d_{[32]}}{\partial x_i}\right)\\ &+ 2\frac{\partial^2 \phi}{\partial m\,\partial d_{[12]}^2}d_{[12]}\frac{\partial d_{[12]}}{\partial x_i}\Bigg].\end{aligned} \tag{26}$$

In view of eqn (25), z_i will depend on

$$\frac{\partial^2 \phi_0}{\partial m^2}, \quad \frac{\partial^2 \phi_0}{\partial m\,\partial(d_{[31]}^2 + d_{[32]}^2)}, \quad \frac{\partial^2 \phi_0}{\partial m\,\partial d_{[12]}^2},$$

and on

$$\frac{\partial^2 B_i}{\partial m^2}, \quad \frac{\partial^2 B_i}{\partial m\,\partial(d_{[31]}^2 + d_{[32]}^2)}, \quad \frac{\partial^2 B_i}{\partial m\,\partial d_{[12]}^2}$$

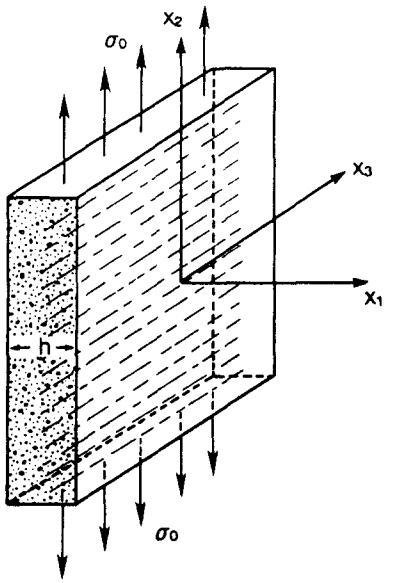

Fig. 3. The geometry of a unidirectionally reinforced coupon, with fibers in the x_3-direction, diffusion in the x_1-direction and load in the x_2-direction.

($i = 1, \ldots, 4$) as well as on terms like

$$\frac{\partial B_3}{\partial m}\frac{\partial D}{\partial x_i}, \text{etc.}$$

In view of the dependence of $P_1, P_6, \ldots, r_{13}$ in eqns (19) on σ_{ij} it follows that $d_{[ij]}$ may introduce a non-linear stress effect on z_i. However, for sufficiently short times—when $d_{[ij]}$ remain relatively small—it is plausible to expect that for $\sigma_{ij}/\sigma_f \ll 1$, z_i will be linear in σ_{ij}.

8. A SPECIAL SUB CASE: UNIDIRECTIONAL DIFFUSION UNDER A CONSTANT TRANSVERSE LOAD

Consider a unidirectionally reinforced plate of thickness h, with fibers parallel to the x_3-axis, subjected to a constant stress $\sigma_{22} = \sigma_0$ with diffusion in the x_1-direction, as shown in Fig. 3.

In view of the observation that most damage due to moisture occurs at the fiber–matrix interfaces†[9, 16, 17, 35] assume $d_{[12]} = 0$. Furthermore, assume gradients only in the x_1-direction. Then, by eqn (26), $z_2 = z_3 = 0$.

In these circumstances eqn (24) gives

$$\varepsilon_i = S_{i0} + S_{i2}\sigma_0 \quad (i = 1, 2, 3, 6), \qquad \text{while} \quad \varepsilon_4 = \varepsilon_5 = 0.$$

In addition, eqns (18), (19), (25) and (26) yield:

damage growth rates

$$\phi_{[32]} = r_1 d_{[32]} - r_4 z_1^2 d_{[32]} \tag{27a}$$

$$\phi_{[31]} = r_1 d_{[31]} + r_4 z_1^2 d_{[31]}; \tag{27b}$$

† See also Fig. 8.

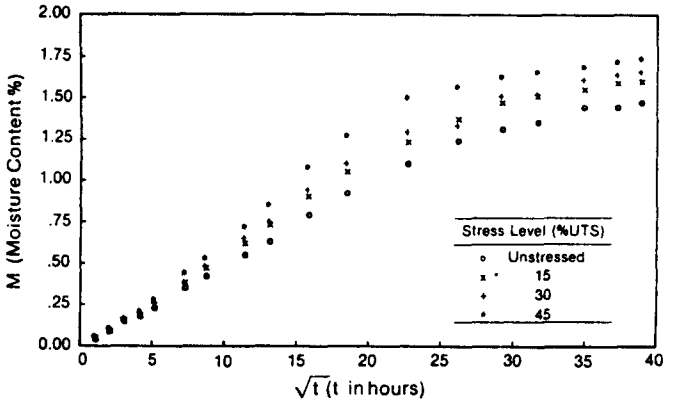

Fig. 4. Average moisture content as a function of $\sqrt{\text{time}}$ in AS4/3502 graphite/epoxy coupons subjected to various stress levels during absorption (97% relative humidity and 40°C).

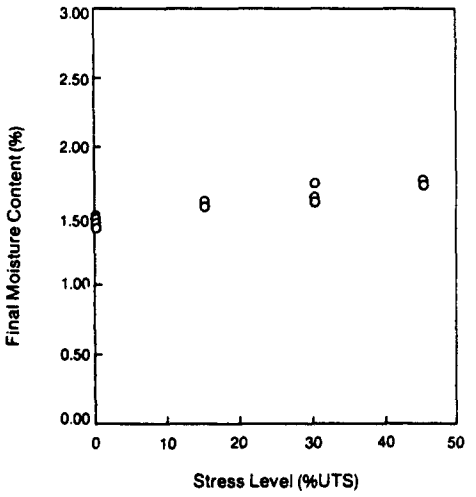

Fig. 5. Maximum moisture content obtained in absorption as a function of the applied stress for AS4/3502 graphite/epoxy coupons.

moisture fluxes

$$f_1 = P_1 z_1 + P_6 D z_1 \tag{28a}$$

$$f_2 = 2P_6 d_{[31]} d_{[32]} z_1 ; \tag{28b}$$

chemical potential and its gradient

$$\tilde{\mu} = \frac{\partial \phi_0}{\partial m} - \frac{\partial B_2}{\partial m}\left(\frac{\sigma_0}{\sigma_f}\right) + \frac{\partial B_3}{\partial m} D\left(\frac{\sigma_0}{\sigma_f}\right) + O(\sigma_0/\sigma_f)^2 \tag{29a}$$

$$z_1 = R_1 \frac{\partial m}{\partial x_1} + R_2 \frac{\partial D}{\partial x_1} + R_3 \frac{\partial (d_{[31]}^2 + d_{[32]}^2)}{\partial x_1} + O(\sigma_0/\sigma_f)^2 \tag{29b}$$

where

$$R_1 = \frac{\partial^2 \phi_0}{\partial m^2} - \frac{\partial^2 B_2}{\partial m^2}\left(\frac{\sigma_0}{\sigma_f}\right) + \frac{\partial^2 B_3}{\partial m^2} D\left(\frac{\sigma_0}{\sigma_f}\right), \quad R_2 = \frac{\partial B_3}{\partial m}\left(\frac{\sigma_0}{\sigma_f}\right),$$

$$R_3 = \frac{\partial^2 \phi_0}{\partial m \, \partial (d_{[31]}^2 + d_{[32]}^2)} - \frac{\partial^2 B_2}{\partial m \, \partial (d_{[31]}^2 + d_{[32]}^2)}\left(\frac{\sigma_0}{\sigma_f}\right)$$

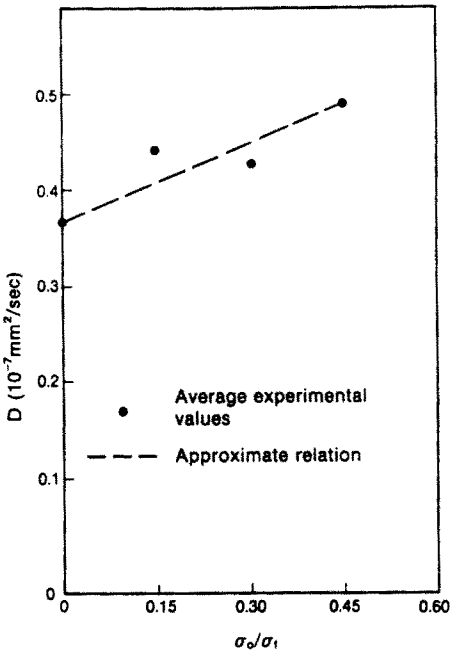

Fig. 6. Variation of the "equivalent Fickian" moisture-diffusivity coefficient D with stress.

$$+\frac{\partial^2 B_3}{\partial m\,\partial(d_{[31]}^2+d_{[32]}^2)}D\left(\frac{\sigma_0}{\sigma_f}\right).$$

In the present circumstances r_1, r_4, P_1, and P_6 in eqns (27) and (28) depend on the following six terms: $\{\sigma_0, d_{[31]}^2+d_{[32]}^2, z_1^2, \sigma_0 D, \sigma_0 z_1^2, z_1^2 D\}$† as well as on m. The quantities ϕ_0, B_2, and B_3 in eqn (29a) depend on $d_{[31]}^2+d_{[32]}^2$ and on m.

In eqns (28) and (29) and the above $D = d_{[31]}^2 - d_{[32]}^2$ as before.

In view of eqns (28) and (29b) the process of moisture transport involves a moisture, stress and damage affected diffusivity. Perhaps more significantly, the terms $\partial(d_{[31]}^2+d_{[32]}^2)/\partial x_1$ and $\partial D/\partial x_1$ in eqn (29b) indicate that sorption is influenced by damage *gradients* which "channel" moisture in the direction of increasing damage. Equations (29)

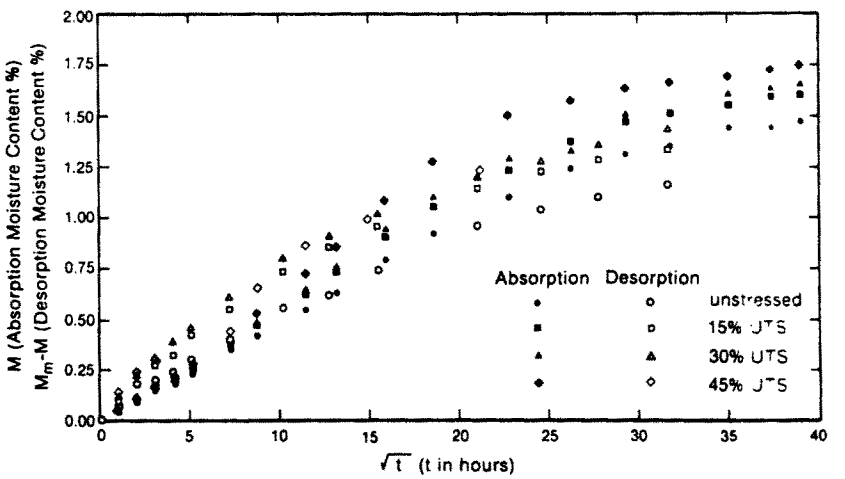

Fig. 7. Superimposed values of moisture content M during absorption and $M-M_m$ during desorption (M_m is the maximum absorbed content) vs $\sqrt{}$time in unidirectional AS4/3502 graphite/epoxy coupons showing the hysteresis loops at various stress levels. Loads applied transversely to fiber direction. Absorption at 97% relative humidity, desorption at 0% relative humidity (all tests at a temperature of 40°C).

† Recall, however, the qualifying statement following eqn (18).

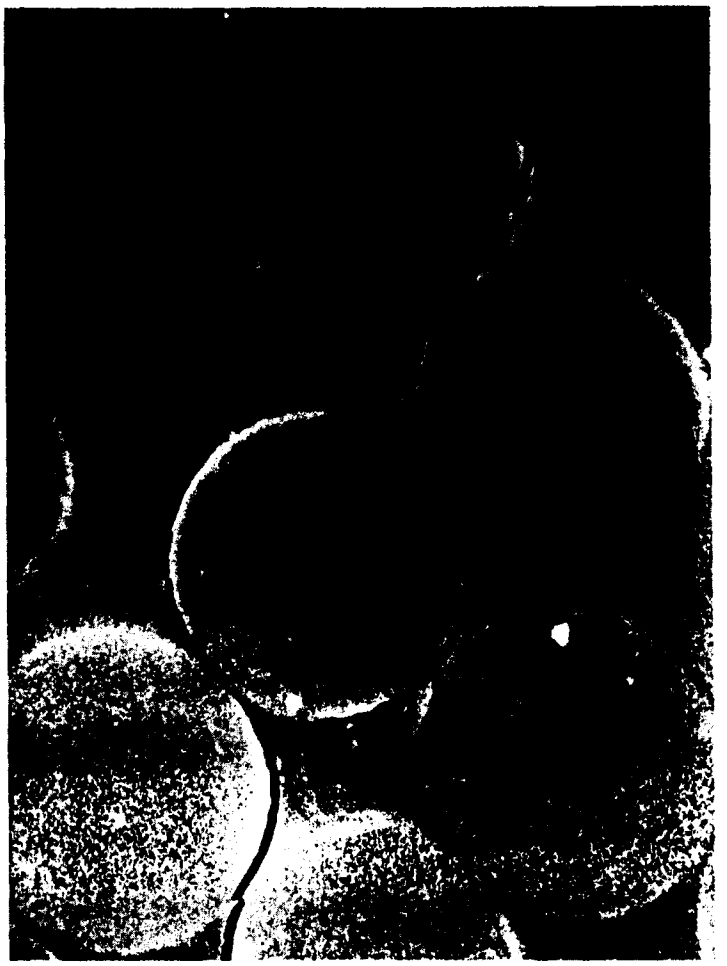

Fig. 8. A scanning electron microscope photograph, showing typical debondings at the fiber–matrix interfaces due to moisture in AS4/3502 graphite/epoxy composite.

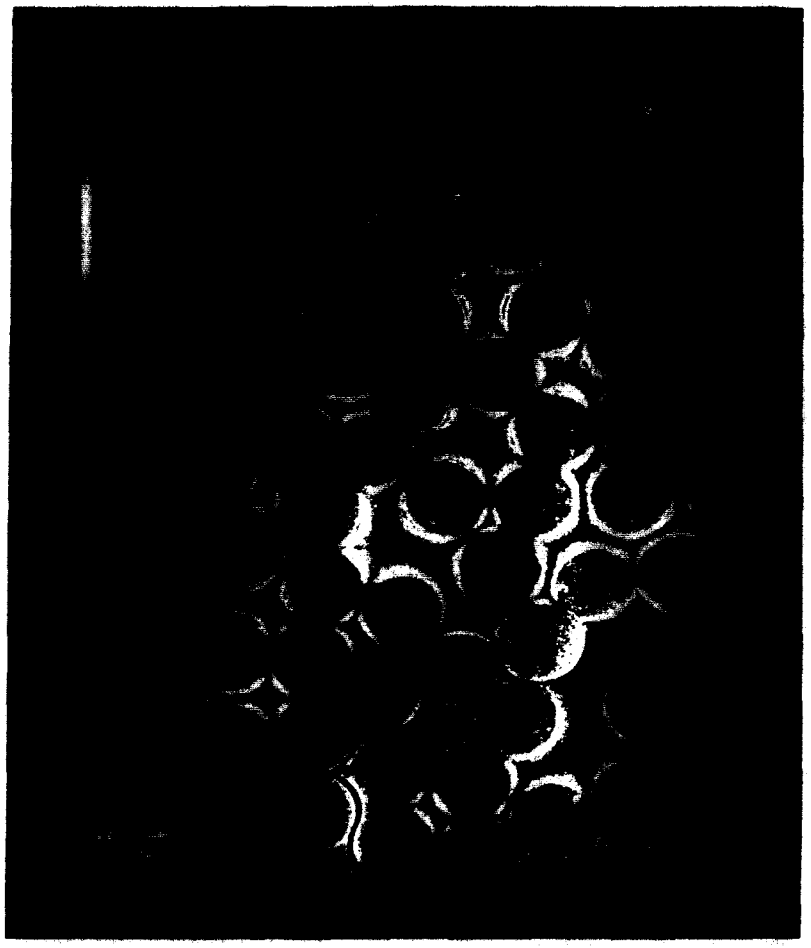

Fig. 9. Profuse microcracking, with some crack coalescence, in an initially saturated, unidirectional AS4/3502, graphite/epoxy laminate exposed to three cycles of 65 and 95% relative humidity, at 24-day intervals. Photograph taken after the third exposure to 65% relative humidity.

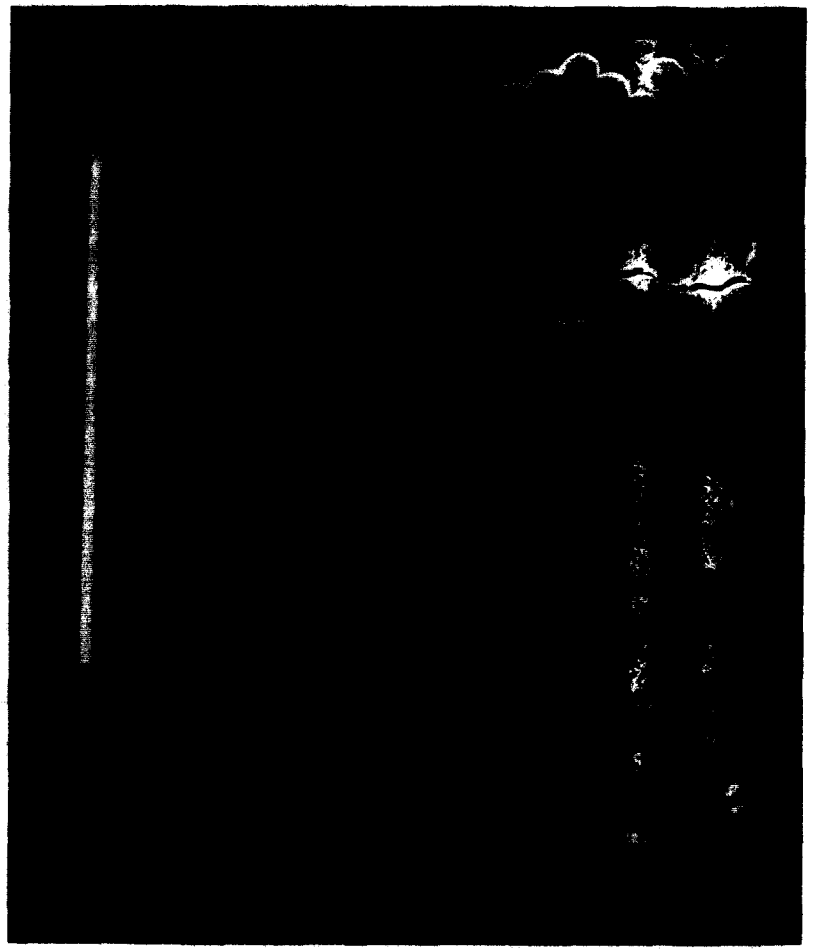

Fig. 10. Microcrack coalescence in an initially dry, unidirectional AS4/3502, graphite/epoxy laminate exposed to nine cycles of 0 and 95% relative humidity at 24-day intervals.

indicate that $\tilde{\mu}$ depends linearly on stress and that such linear dependence is likely to occur also for the diffusivity, at least for early stages of damage development.

The boundary condition on moisture content is determined by

$$\tilde{\mu}(x_1 = \pm h/2, t) = \mu_A \tag{30}$$

where μ_A is the chemical potential of the ambient vapor. For small concentration levels it is plausible to assume that $\tilde{\mu}$ is linearly related to m, whereby eqn (29a) predicts saturation levels which, at least for early stages of damage growth, depend linearly on the stress σ_0.

An experimental investigation of stress-assisted diffusion in AS4/3502 graphite/epoxy coupons was concluded recently[36]. Unidirectionally reinforced specimens were exposed to a constant relative humidity of 97%, at a temperature of 40°C, and loaded transversely to the fiber directions at 0, 15, 30, and 45% of the ultimate stress (where $\sigma_f \simeq 7500$ psi $\simeq 51.7$ MPa). Total moisture weight-gains were recorded periodically in several replicate specimens and results for the average values are shown in Fig. 4. Note the "sigmoidal" shape of all absorption curves, which differs qualitatively from predictions of classical diffusion and indicates a non-linear, concentration-dependent transport process.

The dependence of the maximal moisture content and of the diffusivity on stress are shown in Figs 5 and 6. It can be seen that an approximately linear relationship exists between stress and both of the above quantities, as inferred by the present model.

Moisture weight-losses were measured during desorption at all the above stress levels. These measurements were performed after removing all test coupons from the humid chambers into a dry environment at 0% relative humidity. The resulting weight losses are plotted vs $\sqrt{t}$ in Fig. 7, where the weight-gain data are superimposed for each stress level for the purpose of comparison. Note the substantial hysteresis loops, which can be attributed either to the concentration dependence of the transport process or to the growth of damage, or to both.

9. MOISTURE INDUCED DAMAGE IN THE ABSENCE OF EXTERNAL STRESS

Consider an unstressed unidirectionally reinforced plate, of thickness h as before with all fibers parallel to the x_3-axis and moisture diffusion in the x_1-direction. In this case eqns (27) and (28) remain unchanged, except that r_1, r_4, P_1 and P_6 depend only on $d^2_{[31]}+d^2_{[32]}$, m (and possibly z^2_1).

Equations (29) reduce to

$$\tilde{\mu} = \frac{\partial \phi_0}{\partial m} \tag{31a}$$

and

$$z_1 = \frac{\partial^2 \phi_0}{\partial m^2}\frac{\partial m}{\partial x_1} + \frac{\partial^2 \phi_0}{\partial m\, \partial (d^2_{[31]}+d^2_{[32]})}\frac{\partial (d^2_{[31]}+d^2_{[32]})}{\partial x_1}. \tag{31b}$$

In view of eqns (27) and (31b) it is clear that damage growth rate depends on the extent of existing damage and that this rate may also depend on moisture content and the magnitude of the moisture gradient. A dependence of $\phi_{[ij]}$ on $d_{[ij]}$ would lead to a synergistic effect which accentuates damage localization ("damage breeds upon itself"). A dependence of $\phi_{[ij]}$ upon $|\partial m/\partial x_i|$ would tend to localize the damage in places of highest moisture gradients, namely near the boundaries $x_1 = \pm h/2$.

The typical form of moisture induced damage is shown in Fig. 8. Note the "damage" occurs as debondings at the fiber–matrix interfaces. Initially, these debondings appear as isolated interfacial crescents. Upon repeated absorption/desorption cycles these crescents grow, until they coalesce to create highly localized damage in the form of continuous cracks. Typical forms of such cracks are shown in Figs 9 and 10[37, 38].

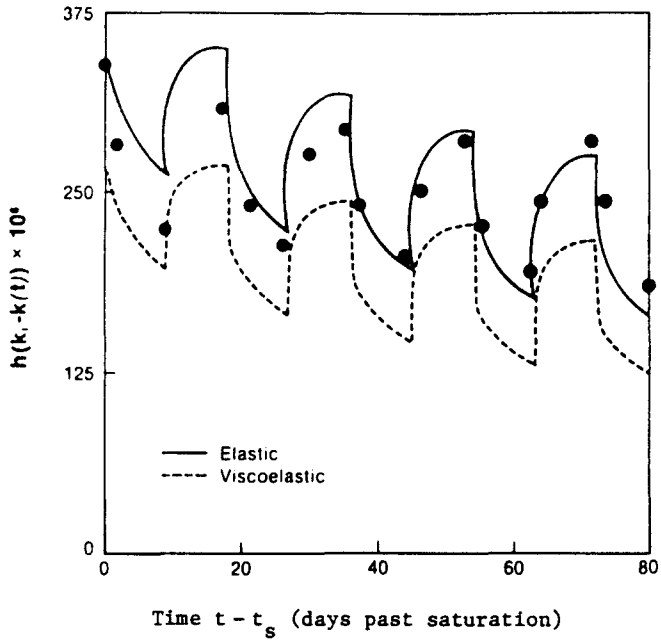

Fig. 11. Time-dependent curvature change of $(0/90/0_4/90_4/0/90)_T$ AS4/3502 graphite/epoxy laminates during cyclic exposure to 0 and 95% relative humidities at 130°F, with cycle interval of 9 days.

The growth of damage can be inferred also from weight-gain and curvature measurements in anti-symmetric, cross-ply composite plates[17, 39]. Due to the anti-symmetry of the lay-up, these plates deform into saddle shaped surfaces upon cool-down from the elevated cure temperature, with initial curvatures $k_x = -k_y = k_i$. Upon subsequent exposure to moisture, these curvatures vary with time, whereby $k = k(t)$. The variation of $k_i - k(t)$ vs time is shown in Figs 11 and 12, where experimental results are compared against theoretical predictions of linear elasticity and linear viscoelasticity. (In those figures h denotes plate thickness and in Fig. 11 t_s denotes the time required to saturate initially dry plates, prior to their exposure to cyclic ambient humidities.)

The variation of the total moisture content M vs time in the anti-symmetric cross-ply plates is shown in Figs 13 and 14. Weight-gain data points are shown in comparison with predictions of classical diffusion theory ("Fick's law").

Inspection of Figs 11–14 shows increasing departures between data and theoretical computations. These departures are most likely attributable to the presence and growth of damage, which was not incorporated into the theoretical analyses and predictions of Refs [17, 39]. The growth and location of damage in the anti-symmetric plates, in relation to the moisture–exposure history, is sketched in Fig. 15.

The experimental observations exhibited in Figs 8–14, as well as in Figs 4, 5 and 7, support qualitatively the general trends of the damage theory developed in this paper.

10. CONCLUSIONS

A continuum damage model was developed for a unidirectionally reinforced, polymeric-resin composite that absorbs moisture from a humid ambient environment. Damage was interpreted as the total cross-sectional area of microcracks that occur within a characteristic material cell prior to the formation of a dominant crack. The total microcracked area was nondimensionalized through division by the respective areas of the cell's walls and was represented by a skew-symmetric, second rank, tensor valued, internal state variable.

Moisture ingress into the composite was treated in the context of the thermodynamics of open system and coupled moisture, stress and damage relations were derived from fundamental principles of thermodynamics and continuum mechanics. These relations

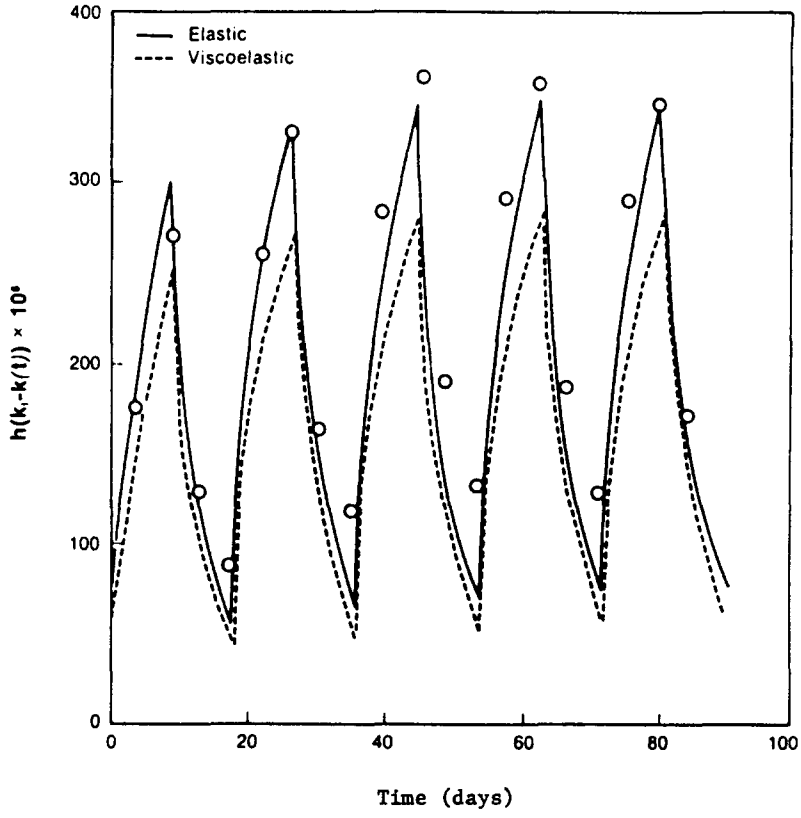

Fig. 12. Time-dependent curvature change of $(0/90/0_4/90_4/0/90)_T$ AS4/3502 graphite/epoxy laminates during cyclic exposure to 0 and 95% relative humidities at 150°F, with cycle interval of 9 days.

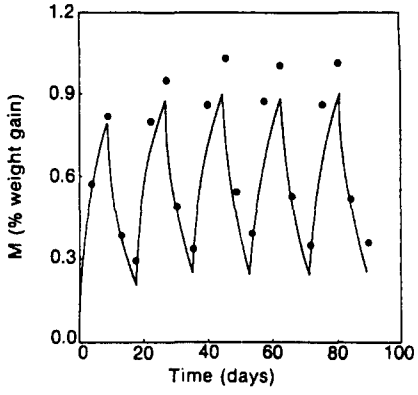

Fig. 13. Moisture content (in % weight gain) during cyclic exposure to 0 and 95% relative humidities at 150°F, with cycle interval of 9 days.

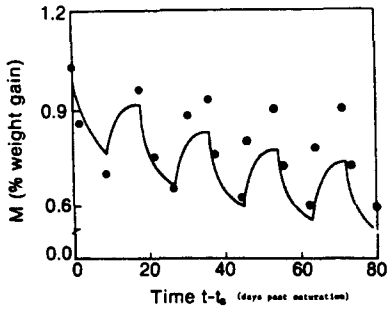

Fig. 14. Moisture content (in % weight gain) during cyclic exposure to 0 and 95% relative humidities at 130°F, with cyclic interval of 9 days.

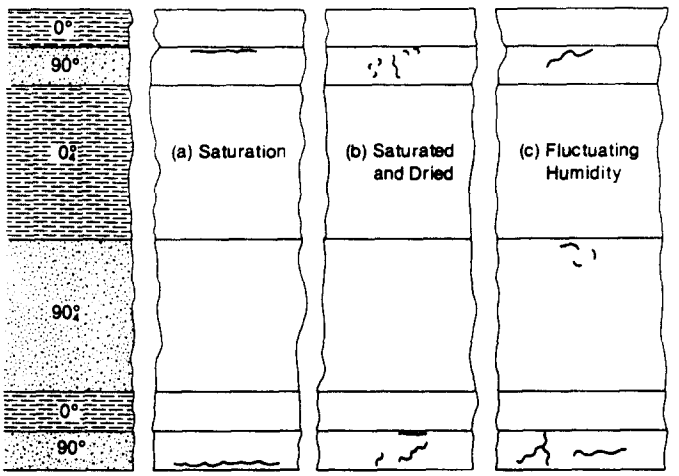

Fig. 15. A sketch of damage progression in a $[0/90/0_4/90_4/0/90]_T$ AS4/3502 graphite/epoxy laminate with exposure to moisture. Shown at each stage are damage patterns that developed *in addition* to previous damage.

included formal expressions for the evolution of damage, for stress-and-damage-coupled diffusion, as well as for damage-dependent material compliances.

It was shown that experimental observations of moisture-induced damage, and of moisture absorption and desorption in the presence and absence of stress, tended to verify some of the salient aspects featured in the continuum damage model proposed in this work.

The present work did not provide explicit expressions for the evolution of damage or any of the other formal relations. This deficiency is due to the paucity in data that are available at the present time. Specifically, while several hypotheses for the prime causes of moisture-induced debondings at fiber–matrix interfaces have been proposed (see, e.g. Ref. [38]), the exact mechanism is not yet clear and cannot be modelled by fracture mechanics. Furthermore, observations of moisture-induced damage are still scarce and inconclusive. Like all fatigue and damage phenomena they exhibit extensive variation and scatter. A larger data base for damage and a basic physio-chemical understanding of the debonding process are necessary for further progress in this subject.

Acknowledgement—The author wishes to express his sincere thanks to Profs A. C. Pipkin of Brown University and A. J. M. Spencer of the University of Nottingham for most helpful discussions. This investigation was conducted under Contract N00014-82-K-0562 from the Office of Naval Research (ONR). The author is grateful to Dr Y. Rajapakse of the Mechanics Division, Engineering Sciences Directorate, ONR, for his support and encouragement.

REFERENCES

1. B. D. Coleman and M. E. Gurtin, Thermodynamics with internal state variables. *J. Chem. Phys.* **47**(2), 597–613 (1967).
2. J. Bataille and J. Kestin, Irreversible processes and physical interpretation of rational thermodynamics. *J. Non-Equil. Thermodyn.* **4**, 229–258 (1979).
3. D. Krajcinovic, Continuum damage mechanics. *Appl. Mech. Rev.* **37**(1), 1–6 (Jan. 1984).
4. R. Talreja, Transverse cracking and stiffness reduction in composite laminates. *J. Comp. Mater.* **19**, 355–375 (July 1985).
5. R. Talreja, A continuum mechanics characterization of damage in composite materials. *Proc. R. Soc. London* **A399**, 195–216 (1985).
6. D. Krajcinovic, Continuum damage mechanics revisited : basic concepts and definitions. *J. Appl. Mech.* **52**(4), 829–834 (1985).
7. L. Davison and A. L. Stevens, Thermomechanical constitution of spalling bodies. *J. Appl. Phys.* **44**, 667–674 (1973).
8. J. P. Komorowski, Hygrothermal effects in continuous fibre reinforced composites. Aeronautical Notes NAE-AN-4, 10, 11, and 12, National Research Council Canada (1983).
9. K. H. G. Ashbee and R. C. Wyatt, Water damage in glass fibre/resin composites. *Proc. R. Soc. London* **A312**, 553–564 (1969).

10. I. G. Hedrick and J. B. Whiteside, Effects of environment on advanced composite structures. AIAA Conference on Aircraft Composites, San Diego, California, 24–25 March 1977 (paper 77-463).
11. R. J. DeIasi, J. B. Whiteside and W. Wolter, Effects of varying hygrothermal environments on moisture absorption in epoxy composites. *Proc. Army, Air Force, Navy, NASA Fourth Conf. on Fibrous Composites in Structural Design*, San Diego, California, 13–17 Nov. 1978.
12. C. D. Shirrell, W. H. Leisler and F. A. Sandow, Moisture-induced surface damage in T300/5208 graphite/epoxy laminates. In *Nondestructive Evaluation and Flaw Criticality for Composite Materials* (Edited by R. B. Pipes), ASTM STP 696, pp. 209–222 (1979).
13. F. W. Crossman, R. E. Mauri and W. J. Warren, Hygrothermal damage mechanisms in graphite–epoxy composites. Lockheed Palo Alto Research Laboratory, Final Report (December 1979).
14. C. L. Leung and D. H. Kaelble, Moisture diffusion and microdamage in composites. *ASC Symp. Ser.* **1980**(132), 419–434 (1980).
15. M. K. Antoon and J. L. Koenig, Irreversible effects of moisture on the epoxy matrix in glass-reinforced epoxy composites. *J. Polym. Sci.: Polym. Phys. Edn* **19**, 197–212 (1981).
16. L. T. Drzal, M. J. Rich and M. F. Koenig, Adhesion of graphite fibers to epoxy matrices, III: the effect of hygrothermal exposure. *J. Adhesion* **18**, 49–72 (1985).
17. S. P. Jackson and Y. Weitsman, Moisture effects and moisture induced damage in composites. *Proceedings of the Fifth International Conference on Composite Materials* (ICCM V), San Diego, California, 30 July–1 Aug. 1985, pp. 1435–1452.
18. V. P. Gupta, L. T. Drzal and M. J. Rich, The physical basis of moisture transport in a cured epoxy resin system. *J. Appl. Polym. Sci.* **30**, 4467–4493 (1985).
19. M. A. Biot, General theory of three-dimensional consolidation. *J. Appl. Phys.* **12**, 155–164 (1941).
20. M. A. Biot, Theory of finite deformations of porous solids. *Indiana Univ. Math. J.* **21**(7), 597–620 (1972).
21. M. A. Biot, Nonlinear and semilinear rheology of porous solids. *J. Geophys. Res.* **78**(23), 4924–4937 (1973).
22. M. E. Gurtin, On the linear theory of diffusion through an elastic solid. *Proc. Conf. on Environmental Degradation of Engineering Materials*, Virginia Tech, 10–12 Oct. 1977, pp. 107–119.
23. J. Kestin, *A Course in Thermodynamics*, Vol. I, pp. 582–585. McGraw-Hill, New York (1979).
24. J. R. Rice and M. P. Cleary, Some basic stress diffusion solutions for fluid-saturated elastic porous media with compressible constituents. *Rev. Geophys. Space Phys.* **14**(2), 227–241 (1976).
25. R. D. Jamison, K. Schulte, K. L. Reifsnider and W. W. Stinchcomb, Characterization and analysis of damage mechanisms in tension–tension fatigue of graphite/epoxy laminates. In *Effects of Defects in Composite Materials* (D. J. Wilkins, Symposium Chairman), ASTM STP 836, pp. 21–55. ASTM (1984).
26. A. L. Highsmith, W. W. Stinchcomb and K. L. Reifsnider, Effect of fatigue-induced defects on the residual response of composite laminates. In *Effects of Defects in Composite Materials* (D. J. Wilkins, Symposium Chairman), ASTM STP 836, pp. 194–216. ASTM (1984).
27. Y. Weitsman, Environmentally induced damage in composites. *Proc. of the 5th Int. Symp. on "Continuum Models for Discrete Systems"* (Edited by A. J. M. Spencer), pp. 187–192. A. A. Balkema, Rotterdam, Holland (1987).
28. W. Jaunzemis, *Continuum Mechanics*, pp. 286–288. Macmillan, New York (1967).
29. Y. C. Fung, *Foundations of Continuum Mechanics*, pp. 436–439. Prentice Hall, Englewood Cliffs, New Jersey (1965).
30. G. F. Smith, On transversely isotropic functions of vectors symmetric second-order and skew-symmetric second order tensors. *Q. Appl. Math.* **39**, 509–516 (1982).
31. A. C. Pipkin and R. S. Rivlin, The formulation of constitutive equations in continuum physics. I. *Archs Ration. Mech. Analysis* **4**, 129–144 (1959).
32. A. J. M. Spencer, *"Theory of Invariants" in Continuum Physics* (Edited by A. C. Eringen), Vol. 1, pp. 239–353. Academic Press, New York (1971).
33. I. Prigogine, *Thermodynamics of Irreversible Processes*, 3rd Edn, pp. 93–94. Interscience (1967).
34. Y. Weitsman, Stress assisted diffusion in elastic and viscoelastic materials. *J. Mech. Phys. Solids* **35**(1), 73–97 (1987).
35. J. W. Rock and F. R. Jones, Nucleation and crack growth in GRP under stress corrosion conditions. *Proceedings of the Fifth International Conference on Composite Materials* (ICCM V), San Diego, California, 30 July–1 Aug. 1985, pp. 1453–1462.
36. M. C. Henson and Y. Weitsman, Stress effects on moisture transport in an epoxy resin and its composite. *Proc. 3rd Japan–U.S. Conf. on Composite Materials*, Tokyo, June 1986 (Edited by K. Kawata, S. Umekawa and A. Kobayashi), pp. 775–784.
37. G.-P. Fang, Moisture and temperature effects in composite materials, M.Sc. thesis, Texas A&M University, Nov. 1986 (Texas A&M University Report MM-5022-86-21).
38. Y. Weitsman, Moisture in composites: sorption and damage. *Fatigue in Composites* (Edited by K. L. Reifsnider). Elsevier Science, New York (1987), in press.
39. B. D. Harper and Y. Weitsman, On the effects of environmental conditioning on residual stresses in composite laminates. *Int. J. Solids Structures* **21**, 907–926 (1985).

APPENDIX: TRANSVERSE ISOTROPY, T-4 SYMMETRY (ABOUT X_3-AXIS)

Case of one symmetric tensor A_{ij}, one anti-symmetric tensor W_{ij}, and one vector V_i

(I) *Invariants*

$$I_1 = A_{33}, \quad I_2 = A_{11}+A_{22}, \quad I_3 = (A_{11}-A_{22})^2+4A_{12}^2, \quad I_4 = A_{31}^2+A_{32}^2, \quad I_5 = W_{31}^2+W_{32}^2,$$

$$I_6 = A_{31}W_{31}+A_{32}W_{32}, \quad I_7 = V_1^2+V_2^2, \quad I_8 = V_3^2, \quad I_9 = W_{12}^2,$$

$$\begin{bmatrix} I_{10} \\ I_{11} \\ I_{12} \end{bmatrix} = (A_{11}-A_{22})\begin{bmatrix} A_{31}^2-A_{32}^2 \\ A_{31}W_{31}-A_{32}W_{32} \\ W_{31}^2-W_{32}^2 \end{bmatrix} + 2A_{12}\begin{bmatrix} 2A_{31}A_{32} \\ A_{31}W_{32}+A_{32}W_{31} \\ 2W_{31}W_{32} \end{bmatrix}$$

$$I_{13} = (A_{11}-A_{22})(V_1^2-V_2^2)+4A_{12}V_1V_2,$$

$$\begin{bmatrix} I_{14} \\ I_{15} \\ I_{16} \end{bmatrix} = (V_1^2-V_2^2)\begin{bmatrix} A_{31}^2-A_{32}^2 \\ A_{31}W_{31}-A_{32}W_{32} \\ W_{31}^2-W_{32}^2 \end{bmatrix} + 2V_1V_2\begin{bmatrix} 2A_{31}A_{32} \\ A_{31}W_{32}+A_{32}W_{31} \\ 2W_{31}W_{32} \end{bmatrix}$$

$$\begin{bmatrix} I_{17} \\ I_{18} \end{bmatrix} = V_3\begin{bmatrix} A_{31}V_1+A_{32}V_2 \\ W_{31}V_1+W_{32}V_2 \end{bmatrix}, \qquad I_{19} = W_{12}(A_{31}W_{32}-A_{32}W_{31}),$$

$$I_{20} = [(A_{11}-A_{22})V_1V_2-A_{12}(V_1^2-V_2^2)](A_{31}W_{32}-A_{32}W_{31}),$$

$$\begin{bmatrix} I_{21} \\ I_{22} \\ I_{23} \end{bmatrix} = W_{12}\left\{(A_{11}-A_{22})\begin{bmatrix} 2A_{31}A_{32} \\ A_{31}W_{32}+A_{32}W_{31} \\ 2W_{31}W_{32} \end{bmatrix} - 2A_{12}\begin{bmatrix} A_{31}^2-A_{32}^2 \\ A_{31}W_{31}-A_{32}W_{32} \\ W_{31}^2-W_{32}^2 \end{bmatrix}\right\}$$

$$I_{24} = W_{12}[(A_{11}-A_{22})V_1V_2-A_{12}(V_1^2-V_2^2)]$$

$$\begin{bmatrix} I_{25} \\ I_{26} \\ I_{27} \end{bmatrix} = W_{12}\left\{2\begin{bmatrix} A_{31}^2-A_{32}^2 \\ A_{31}W_{31}-A_{32}W_{32} \\ W_{31}^2-W_{32}^2 \end{bmatrix}V_1V_2 - \begin{bmatrix} 2A_{31}A_{32} \\ A_{31}W_{32}+A_{32}W_{31} \\ 2W_{31}W_{32} \end{bmatrix}(V_1^2-V_2^2)\right\}$$

$$\begin{bmatrix} I_{28} \\ I_{29} \end{bmatrix} = V_3\left\{(A_{11}-A_{22})\begin{bmatrix} A_{31}V_1-A_{32}V_2 \\ W_{31}V_1-W_{32}V_2 \end{bmatrix} + 2A_{12}\begin{bmatrix} A_{31}V_2+A_{32}V_1 \\ W_{31}V_2+W_{32}V_1 \end{bmatrix}\right\}$$

$$\begin{bmatrix} I_{30} \\ I_{31} \end{bmatrix} = V_3W_{12}\begin{bmatrix} A_{31}V_2-A_{32}V_1 \\ W_{31}V_2-W_{32}V_1 \end{bmatrix}$$

$$\begin{bmatrix} I_{32} \\ I_{33} \end{bmatrix} = V_3W_{12}\left\{(A_{11}-A_{22})\begin{bmatrix} A_{31}V_2+A_{32}V_1 \\ W_{31}V_2+W_{32}V_1 \end{bmatrix} - 2A_{12}\begin{bmatrix} A_{31}V_1-A_{32}V_2 \\ W_{31}V_1-W_{32}V_2 \end{bmatrix}\right\}.$$

(2) *Vector-valued functions*

$$\begin{aligned} u_1 = {} & P_1V_1+P_2[(A_{11}-A_{22})V_1+2A_{12}V_2]+P_3(A_{31}W_{32}-A_{32}W_{31})V_2 \\ & + \begin{bmatrix} P_4 \\ P_5 \\ P_6 \end{bmatrix}\left\{\begin{bmatrix} A_{31}^2-A_{32}^2 \\ A_{31}W_{31}-A_{32}W_{32} \\ W_{31}^2-W_{32}^2 \end{bmatrix}V_1 + \begin{bmatrix} 2A_{31}A_{32} \\ A_{31}W_{32}+A_{32}W_{31} \\ 2W_{31}W_{32} \end{bmatrix}V_2\right\} + \begin{bmatrix} P_7 \\ P_8 \end{bmatrix}V_3\begin{bmatrix} A_{31} \\ W_{31} \end{bmatrix} + P_9W_{12}V_2 \\ & + \begin{bmatrix} P_{10} \\ P_{11} \\ P_{12} \end{bmatrix}\left\{(A_{11}-A_{22})\begin{bmatrix} 2A_{31}A_{32} \\ A_{31}W_{32}+A_{32}W_{31} \\ 2W_{31}W_{32} \end{bmatrix} - 2A_{12}\begin{bmatrix} A_{31}^2-A_{32}^2 \\ A_{31}W_{31}-A_{32}W_{32} \\ W_{31}^2-W_{32}^2 \end{bmatrix}\right\}V_2 \\ & + P_{13}[(A_{11}-A_{22})V_2-2A_{12}V_1](A_{31}W_{32}-A_{32}W_{31})+P_{14}[(A_{11}-A_{22})V_2-2A_{12}V_1]W_{12} \\ & + \begin{bmatrix} P_{15} \\ P_{16} \\ P_{17} \end{bmatrix}W_{12}\left\{\begin{bmatrix} A_{31}^2-A_{32}^2 \\ A_{31}W_{31}-A_{32}W_{32} \\ W_{31}^2-W_{32}^2 \end{bmatrix}V_2 - \begin{bmatrix} 2A_{31}A_{32} \\ A_{31}W_{32}+A_{32}W_{31} \\ 2W_{31}W_{32} \end{bmatrix}V_1\right\} \\ & + \begin{bmatrix} P_{18} \\ P_{19} \end{bmatrix}V_3\left\{(A_{11}-A_{22})\begin{bmatrix} A_{31} \\ W_{31} \end{bmatrix} + 2A_{12}\begin{bmatrix} A_{32} \\ W_{32} \end{bmatrix}\right\} + \begin{bmatrix} P_{20} \\ P_{21} \end{bmatrix}V_3W_{12}\begin{bmatrix} A_{32} \\ W_{32} \end{bmatrix} \\ & + \begin{bmatrix} P_{22} \\ P_{23} \end{bmatrix}V_3W_{12}\left\{(A_{11}-A_{22})\begin{bmatrix} A_{32} \\ W_{32} \end{bmatrix} - 2A_{12}\begin{bmatrix} A_{31} \\ W_{31} \end{bmatrix}\right\} \end{aligned}$$

$$\begin{aligned} u_2 = {} & P_1V_2+P_2[-(A_{11}-A_{22})V_2+2A_{12}V_1]-P_3(A_{31}W_{32}-A_{32}W_{31})V_1 \\ & + \begin{bmatrix} P_4 \\ P_5 \\ P_6 \end{bmatrix}\left\{-\begin{bmatrix} A_{31}^2-A_{32}^2 \\ A_{31}W_{31}-A_{32}W_{32} \\ W_{31}^2-W_{32}^2 \end{bmatrix}V_2 + \begin{bmatrix} 2A_{31}A_{32} \\ A_{31}W_{32}+A_{32}W_{31} \\ 2W_{31}W_{32} \end{bmatrix}V_1\right\} + \begin{bmatrix} P_7 \\ P_8 \end{bmatrix}V_3\begin{bmatrix} A_{32} \\ W_{32} \end{bmatrix} - P_9W_{12}V_1 \\ & - \begin{bmatrix} P_{10} \\ P_{11} \\ P_{12} \end{bmatrix}\left\{(A_{11}-A_{22})\begin{bmatrix} 2A_{31}A_{32} \\ A_{31}W_{32}+A_{32}W_{31} \\ 2W_{31}W_{32} \end{bmatrix} - 2A_{12}\begin{bmatrix} A_{31}^2-A_{32}^2 \\ A_{31}W_{31}-A_{32}W_{32} \\ W_{31}^2-W_{32}^2 \end{bmatrix}\right\}V_1 \\ & + P_{13}[(A_{11}-A_{22})V_1+2A_{12}V_2](A_{31}W_{32}-A_{32}W_{31})+P_{14}[(A_{11}-A_{22})V_1+2A_{12}V_2]W_{12} \end{aligned}$$

$$+\begin{bmatrix}P_{15}\\P_{16}\\P_{17}\end{bmatrix}W_{12}\left\{\begin{bmatrix}A_{31}^2-A_{32}^2\\A_{31}W_{31}-A_{32}W_{32}\\W_{31}^2-W_{32}^2\end{bmatrix}V_1+\begin{bmatrix}2A_{31}A_{32}\\A_{31}W_{32}+A_{32}W_{31}\\2W_{31}W_{32}\end{bmatrix}V_2\right\}$$
$$+\begin{bmatrix}P_{18}\\P_{19}\end{bmatrix}V_3\left\{-(A_{11}-A_{22})\begin{bmatrix}A_{32}\\W_{32}\end{bmatrix}+2A_{12}\begin{bmatrix}A_{31}\\W_{31}\end{bmatrix}\right\}-\begin{bmatrix}P_{20}\\P_{21}\end{bmatrix}V_3W_{12}\begin{bmatrix}A_{31}\\W_{31}\end{bmatrix}$$
$$-\begin{bmatrix}P_{22}\\P_{23}\end{bmatrix}V_3W_{12}\left\{(A_{11}-A_{22})\begin{bmatrix}A_{31}\\W_{31}\end{bmatrix}+2A_{12}\begin{bmatrix}A_{32}\\W_{32}\end{bmatrix}\right\}$$

$$u_3=H_1V_3+\begin{bmatrix}H_2\\H_3\end{bmatrix}\begin{bmatrix}A_{31}V_1+A_{32}V_2\\W_{31}V_1+W_{32}V_2\end{bmatrix}$$
$$+\begin{bmatrix}H_4\\H_5\end{bmatrix}\left\{(A_{11}-A_{22})\begin{bmatrix}A_{31}V_1-A_{32}V_2\\W_{31}V_1-W_{32}V_2\end{bmatrix}+2A_{12}\begin{bmatrix}A_{31}V_2+A_{32}V_1\\W_{31}V_2+W_{32}V_1\end{bmatrix}\right\}$$
$$+\begin{bmatrix}H_6\\H_7\end{bmatrix}W_{12}\left\{\begin{bmatrix}A_{31}V_2-A_{32}V_1\\W_{31}V_2-W_{32}V_1\end{bmatrix}\right\}$$
$$+\begin{bmatrix}H_8\\H_9\end{bmatrix}W_{12}\left\{(A_{11}-A_{22})\begin{bmatrix}A_{31}V_2+A_{32}V_1\\W_{31}V_2+W_{32}V_1\end{bmatrix}-2A_{12}\begin{bmatrix}A_{31}V_1-A_{32}V_2\\W_{31}V_1-W_{32}V_2\end{bmatrix}\right\}.$$

(3) *Skew-symmetric tensor valued functions*

$$\chi_{31}=r_1W_{31}+r_2[(A_{11}-A_{22})W_{31}+A_{12}W_{32}-A_{32}W_{12}]+r_3V_2(V_1A_{32}-V_3A_{12})$$
$$+r_4[(V_1^2-V_2^2)W_{31}+V_2(V_1W_{32}-V_3W_{12})]+r_5(W_{12}A_{32}-W_{32}A_{12})$$
$$+r_6(A_{11}-A_{12})V_2(V_1A_{32}-V_3A_{12})$$
$$+r_7[(A_{11}-A_{22})V_2(V_1W_{32}-V_3W_{12})-2(V_1^2-V_2^2)(A_{12}W_{32}-A_{32}W_{12})]$$
$$+r_8[(A_{11}-A_{22})(W_{12}A_{32}-W_{32}A_{12})]+r_9W_{12}A_{12}W_{31}$$
$$+r_{10}[(W_{12}A_{32}-W_{32}A_{12})(V_1^2-V_2^2)]+r_{11}W_{12}W_{31}V_1V_2$$
$$+r_{12}V_2(A_{12}V_3-A_{32}V_1)+r_{13}V_2(W_{12}V_3-W_{32}V_1)$$
$$+r_{14}(A_{11}-A_{22})V_2(W_{12}V_3-W_{32}V_1)$$

$$\chi_{32}=r_1W_{32}+r_2[-(A_{11}-A_{22})W_{32}+A_{12}W_{31}-A_{13}W_{21}]+r_3V_1(V_2A_{31}-V_3A_{21})$$
$$+r_4[-(V_1^2-V_2^2)W_{32}+V_1(V_2W_{31}-V_3W_{21})]-r_5(W_{12}A_{31}-W_{13}A_{21})$$
$$-r_6(A_{11}-A_{22})V_1(V_2A_{31}-V_3A_{21})$$
$$-r_7[(A_{11}-A_{22})V_1(V_2W_{31}-V_3W_{21})-2(V_1^2-V_2^2)(A_{12}W_{31}-A_{13}W_{21})]$$
$$+r_8[(A_{11}-A_{22})(W_{12}A_{31}-W_{13}A_{21})]-r_9W_{12}A_{12}W_{32}$$
$$+r_{10}[(W_{12}A_{31}-W_{13}A_{21})(V_1^2-V_2^2)]-r_{11}W_{12}W_{32}V_1V_2$$
$$+r_{12}V_1(A_{12}V_3-A_{13}V_2)-r_{13}V_1(V_3W_{12}-V_2W_{13})$$
$$+r_{14}(A_{11}-A_{22})V_1(W_{12}V_3-W_{13}V_2)$$

$$\chi_{12}=h_1W_{12}+h_2(A_{31}W_{32}-A_{32}W_{31})+h_3V_3(A_{31}V_2-A_{32}V_1)+h_4V_3(W_{31}V_2-W_{32}V_1).$$

ADDENDUM

The following oversight was noted upon reading of proofs, which is corrected below.

Although the invariants I_6, I_{11}, I_{21} and I_{23} are odd in the skew-symmetric tensor W_{ij} their squares and products, namely I_6^2, I_{11}^2, I_{21}^2, I_{23}^2, I_6I_{11}, I_6I_{21}, I_6I_{23}, $I_{11}I_{21}$, $I_{11}I_{23}$ and $I_{21}I_{23}$ can be used in ψ as well as in P_1–P_{23}, H_1–H_9.

For the infinitesimal deformation case in Section 6 it is necessary to consider the contributions of I_6^2, I_{23}^2 and I_6I_{23}, whereby the following terms should be added to eqn (16):

$$\gamma_{14}(\varepsilon_{31}d_{[31]}+\varepsilon_{32}d_{[32]})^2+\gamma_{15}d_{[12]}^2[(\varepsilon_{11}-\varepsilon_{22})d_{[31]}d_{[32]}-\varepsilon_{12}D]^2+\gamma_{17}(\varepsilon_{31}d_{[31]}+\varepsilon_{32}d_{[32]})d_{[12]}[(\varepsilon_{11}-\varepsilon_{22})d_{[31]}d_{[32]}-\varepsilon_{12}D].$$

Consequently, the following terms should be added to the expressions for C_{pq}

$$C_{11}=2\gamma_{15}d_{[12]}d, \quad C_{12}=-2\gamma_{15}d_{[12]}d, \quad C_{14}=\tfrac{1}{2}\gamma_{17}d_{[32]}d$$
$$C_{15}=\tfrac{1}{2}\gamma_{17}d_{[31]}d, \quad C_{16}=-\gamma_{15}d_{[12]}Dd, \quad C_{22}=2\gamma_{15}d_{[12]}d$$
$$C_{24}=-\tfrac{1}{2}\gamma_{17}d_{[32]}d, \quad C_{25}=-\tfrac{1}{2}\gamma_{17}d_{[31]}d, \quad C_{26}=\gamma_{15}d_{[12]}Dd$$
$$C_{44}=\tfrac{1}{2}\gamma_{14}d_{[32]}^2, \quad C_{45}=\tfrac{1}{2}\gamma_{14}d_{[32]}d_{[31]}, \quad C_{46}=-\tfrac{1}{4}\gamma_{17}d_{[32]}d_{[12]}D$$
$$C_{55}=\tfrac{1}{2}\gamma_{14}d_{[31]}^2, \quad C_{56}=-\tfrac{1}{4}\gamma_{17}d_{[31]}d_{[12]}D, \quad C_{66}=\tfrac{1}{2}\gamma_{15}d_{[12]}^2D^2$$

where in the above $d=d_{[12]}d_{[31]}d_{[32]}$.

The expressions for S_{pq} in eqn (24) undergo an analogous modification.